Velocity dependence of free-ion production in K(np)-SF_6 collisions: Internal-to-translational energy transfer

R. A. Popple, M. A. Durham, R. W. Marawar, B. G. Lindsay, K. A. Smith, and F. B. Dunning
Department of Space Physics and Astronomy and the Rice Quantum Institute, Rice University, Houston, Texas 77251
(Received 22 July 1991; revised manuscript received 20 September 1991)

The velocity dependence of the rate constant for free-ion production via the Rydberg electron-transfer reaction $K(np)+SF_6 \rightarrow K^+ + SF_6^{-*}$ has been investigated at intermediate n. The data provide evidence of a postattachment interaction between the product ions in which internal energy from the SF_6^{-*} ion is converted into translational energy. A similar conclusion is reached from measurements of the velocity and angular distributions of the product K^+ ions.

PACS number(s): 34.60.+z, 34.80.Gs

For several years, Rydberg-atom collisions have been used as a tool to investigate electron attachment to electronegative molecules [1–3]. These studies have been predicated on the free-electron model of Rydberg-atom collisions, which asserts that the average separation between the excited, weakly bound electron and the core ion is so large that they can be considered as independent particles. Electron attachment is then viewed as resulting from a binary interaction between the "essentially free" Rydberg electron and target molecule [4]. The free-electron model is reasonable because the range of the electron-target interaction is much smaller than the separation between the Rydberg electron and core ion. The utility and essential correctness of this model have been discussed at length elsewhere [1,4]. However, in performing and interpreting experiments with Rydberg atoms, it is important to understand that the free-electron model can only be expected to apply to the initial Rydberg electron-molecule encounter, after which the reaction products may have some further interaction. Studies with electron-attaching molecules have revealed that, at low-to-intermediate values of principal quantum number n, postattachment electrostatic interactions between the product ions become important and can result in a marked decrease in the rate constant for free-ion production [5–8]. In the present paper we report the findings of a study of the velocity dependence for free-ion production via the reaction

$$K(np)+SF_6 \rightarrow K^+ + SF_6^{-*} , \quad (1)$$

which results in the formation of long-lived SF_6^{-*} ions. The present data provide evidence of a second type of postattachment interaction in which internal energy from the SF_6^{-*} ions is converted into translational energy. This evidence is obtained through measurements of the rate constant for free-ion production and through kinematic studies of the angular and velocity distributions of the product K^+ ions.

The present apparatus is shown in Fig. 1 and has been described previously [2,3]. Potassium atoms contained in a tightly collimated (~1 mm diam) thermal-energy (~300 °C) beam are excited to a selected np state using the output of a frequency-doubled CR699-21 dye laser. The long-term drift in the laser output frequency is reduced to $\lesssim \pm 2$ MHz per day using a technique described in detail elsewhere [9]. The output of the laser is formed into a series of pulses of 1-μsec duration and 5–10-kHz pulse repetition frequency using an acousto-optic modulator. Excitation occurs, in zero field and (typically) in the presence of target gas, near the center of an interaction region defined by two planar fine-mesh grids. Collisions are allowed to occur for a controlled period of time, after which a small pulsed electric field is applied in the interaction region expelling the product ions into time-of-flight mass spectrometers situated above and below the interaction region. Reaction products are identified by both coincidence and time-of-flight techniques: the time-of-flight specifies the product mass and coincidence measurements ensure that the ions detected result from the reaction of interest. One mass spectrometer is equipped with a position-sensitive detector (PSD), which monitors both ion-arrival times and positions. The SF_6^{-*} flight time was typically ~9 μsec. Tests revealed, however, that the SF_6^{-*} signal was independent of flight time (over the range 5–20 μsec) and no evidence of significant SF_6^{-*} decay on the time scale of the present

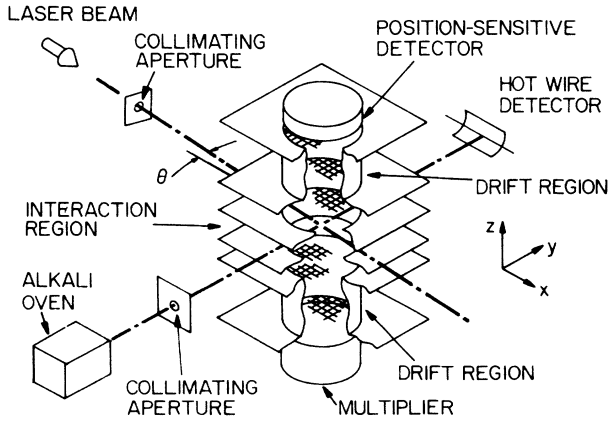

FIG. 1. Schematic diagram of the apparatus.

experiments was detected under any collision conditions.

Velocity-selective Rydberg-atom excitation is achieved by use of Doppler tuning [10]. The laser beam is incident at an angle $\theta \sim 2°$ off normal to the potassium atom beam. For this intersection angle the effective total Doppler width of each excitation line is ~ 200 MHz and is such that, for the range of n of interest in the present work, the Doppler profiles of adjacent states do not overlap. The laser excites atoms in only a small (but stable) segment of the Doppler profile permitting experiments with velocity-selected atoms. The actual width of the velocity distribution of the excited atoms is determined primarily by the divergence of the laser and atom beams.

The velocities of the Rydberg atoms excited were measured directly using the PSD. To accomplish this, pulses of Rydberg atoms were excited with no target gas present. The atoms were then allowed to continue through the interaction region for a predetermined time, typically 10–20 μsec, whereupon they were field ionized [11] by the application of a large pulsed electric field. The resulting K^+ ions are rapidly accelerated by the ionizing field to the PSD and their arrival positions recorded. Analysis of the arrival position distribution gives directly the Rydberg-atom velocity distribution, which typically had a width of $\sim \pm 50$ m sec^{-1}, i.e., approximately one-tenth the width of the Maxwellian distribution of the potassium atom beam. Through such measurements, the relationship between the laser frequency and excited atom velocity can be established. It should be remembered, however, that the target gas molecules are randomly directed and (for SF_6) have a typical velocity of $\sim 2 \times 10^2$ m sec^{-1}. In consequence, the distribution of actual collision velocities is significantly greater than the width of the Rydberg-atom velocity distribution, but this is taken into account in analyzing the data.

Rate constants k_d for Rydberg-atom destruction in collisions with SF_6 were measured first by monitoring the time evolution of the Rydberg-atom population in the interaction region using field ionization. The time evolution of this population is given, to a good approximation, by

$$N(t) = N(0) e^{-t/\tau}, \tag{2}$$

where

$$\frac{1}{\tau} = \frac{1}{\tau_{\text{eff}}} + \rho k_d$$

and $N(0)$ is the number of Rydberg atoms initially present at $t=0$ and τ_{eff} is the effective lifetime of the parent state (taking into account effects due to blackbody radiation). The target gas density ρ (measured using an ionization gauge calibrated against a capacitance manometer) was limited to $< 2 \times 10^{11}$ cm^{-3} to ensure single collision conditions and minimize collisional state changing. The rate constants for such processes are, however, small at low-to-intermediate n due to the relatively large energy separation between the parent np level and other neighboring states [12]. To eliminate the possibility of systematic errors due to multiplier deadtime, the laser power was chosen such that the probability of creating a Rydberg atom during any laser pulse was small (~ 0.05) and the lifetime τ was determined by accumulating data following many laser pulses. Values of k_d were obtained by measuring the inverse lifetime ($1/\tau$) as a function of ρ. The data showed that at $n=19$ (the lowest n at which field ionization could be achieved using available pulsers) the rate constant for collisional destruction was $(3.0 \pm 0.8) \times 10^{-7}$ cm^3 sec^{-1} and, to within experimental error, was independent of relative collision velocity. This is in accord with the free-electron model, which predicts that the rate for Rydberg electron attachment, which is the dominant Rydberg-atom destruction mechanism, will be governed solely by the electron velocity distribution [4].

The velocity dependence of the rate constant for free-ion production was obtained using a somewhat different procedure. As a first step, the Rydberg-atom production rate was measured as a function of Rydberg-atom velocity by observing (with no target gas present) the blackbody-radiation-induced photoion signal produced in some fixed time interval, typically ~ 5 μsec, after excitation [13]. Since the rate for such photoionization is independent of Rydberg-atom velocity, measurement of the K^+ photoion signal as the laser frequency, i.e., Rydberg-atom velocity, is scanned provides the velocity dependence of the Rydberg-atom production rate. Target gas was then introduced and the number of K^+ ions produced through collisions in a time interval of ~ 1 μsec following excitation measured, again as a function of excited atom velocity. (Detection of both the K^+ and SF_6^{-*} products and the use of coincidence techniques permits discrimination against ion signals that do not result from reaction 1.) The velocity dependence of the rate constant for free-ion production was then obtained by taking the ratio, at each velocity, of the collisional and blackbody-radiation-induced ion signals.

Measured rate constants for free-ion production in $K(19p)/SF_6$ collisions are shown in Fig. 2(a) and decrease markedly at low collision velocities. This is not unexpected because, at $n=19$, the positive and negative ions that result from Rydberg electron capture are formed in relatively close proximity and experience strong mutual electrostatic attraction. If the energy available to overcome this attraction comes from the translational energy of the reactants, then as the velocity of the $K(np)$ atoms decreases, so too will the number of product ion pairs that possess sufficient kinetic energy to overcome their mutual attraction and separate, and thus be detected. Therefore, although the rate constant for Rydberg-atom destruction (which proceeds almost entirely through the formation of ion pairs) at $n=19$ is velocity independent, the rate constant for free-ion production is strongly velocity dependent. Figure 2(a), however, also includes the results expected, for the same experimental conditions, on the basis of a Monte Carlo collision model. This model has been described in detail elsewhere [3] and takes into account the velocity distributions of the reactants, the Rydberg electron probability density distribution, and postattachment electrostatic interactions between the product ions. The experimental data and model calculations are normalized at high velocities where postattach-

ment interactions are least important. The observed decrease of the rate constant at low velocities is clearly substantially less than predicted by the model. This discrepancy could arise because of an error in the model or because there is some mechanism not included in the model by which the products gain relative translational energy in the reaction process. If there is indeed such a mechanism, it is likely to involve a postattachment interaction in which internal energy from the (excited) SF_6^{-*} ion is converted into translational energy of the product ion pair. Such an effect would increase the probability that an ion pair can separate and would be most important at low collision velocities where a greater fraction of the product ion pairs is expected to be electrostatically bound. (Internal-to-translational energy transfer might also increase the lifetime of the SF_6^{-*} ions but, as noted earlier, tests revealed no evidence of significant SF_6^{-*} decay on the time scale of the present experiments for any collision velocity.)

To test the validity of the model and the notion of internal-to-translational energy transfer, the velocity dependences of the rate constants for free-ion production in $K(19p)$-CH_3I and $K(19p)$-CF_3I collisions were measured. In each case Rydberg electron transfer results in the formation of short-lived ($\tau \lesssim 1$ psec) intermediate negative ions that dissociate rapidly into an atomic negative ion [14], resulting in the reactions

$$K(19p)+CH_3I \rightarrow K^+ + CH_3I^{-*} \rightarrow K^+ + CH_3 + I^- , \quad (3a)$$

$$K(19p)+CF_3I \rightarrow K^+ + CF_3I^{-*} \rightarrow K^+ + CF_3 + I^- . \quad (3b)$$

Because the intermediate negative ions are very short lived, and because the I^- product is a ground-state atomic ion, there is no opportunity for postattachment transfer of negative-ion internal energy into translation. The experimental data are presented in Figs. 2(b) and 2(c) together with the corresponding model predictions. The data sets are again normalized at the higher energies. In the case of CF_3I, dissociation results in the formation of I^- ions that have appreciable kinetic energies (~ 300 meV) [14] and postattachment interactions are therefore relatively unimportant resulting in only a small velocity dependence in the rate constant for free-ion production. Dissociation of CH_3I^{-*} leads to the formation of I^- ions with much smaller kinetic energies (~ 60 meV) [14] and velocities comparable to those of thermal SF_6 molecules. Postattachment interactions are therefore important and result in a marked reduction in the rate constant for free-ion production at low collision velocities. In both cases, however, the model predictions and experimental data are in very good agreement. Taken together, these data show that the model works well in cases where there is both little (CF_3I) and substantial (CH_3I) postattachment interaction. Thus the discrepancy noted with SF_6 must result from some effect not included in the model, such as internal-to-translational energy transfer. Indeed, model calculations in which only ~ 20 meV of energy is arbitrarily added to the relative kinetic energy of the product ions result in a predicted velocity dependence that is very similar to that observed experimentally.

To further test the hypothesis of postattachment collisional energy interchange, the velocity and angular distributions of the K^+ ions produced in collisions with SF_6 were studied, again using the apparatus shown. Following $K(np)$ excitation, collisions were allowed to occur for a short time interval (~ 1 μsec) after which a pulsed electric field was used to extract any product K^+ ions from the interaction region. These then drifted through the upper mass spectrometer and were detected by the PSD. The SF_6^{-*} ions traversed the lower mass spectrometer. K^+-ion-arrival-position distributions were built up by accumulating data following many laser excitation pulses and time-of-flight and coincidence techniques were used to ensure that the detected ions resulted from the reaction of interest. (The probability that an ion pair would be created following any laser pulse was maintained small, $\lesssim 0.05$, to ensure that two ions would not arrive simultaneously at the PSD, as this would result in a spurious position output.) Because the collision volume and time are well localized, each ion-arrival position recorded reflects the product of the ion drift time to the

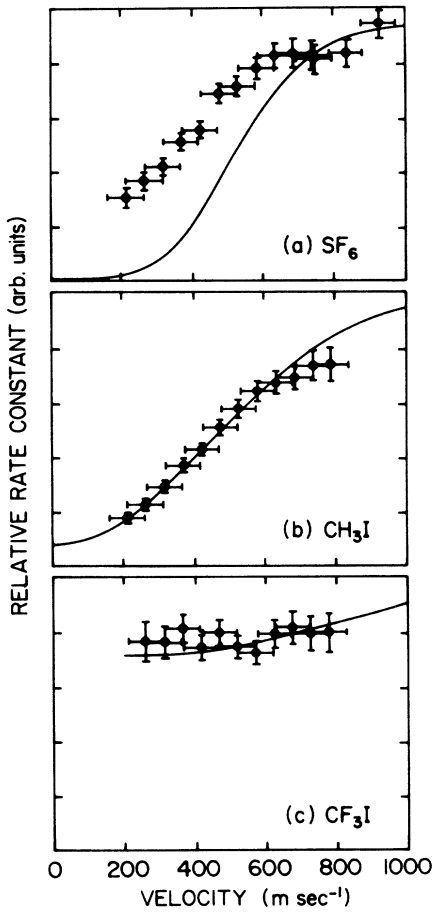

FIG. 2. Rate constants for the production of free ions in collisions between $K(19p)$ atoms and (a) SF_6, (b) CH_3I, and (c) CF_3I as a function of Rydberg-atom velocity. The horizontal bars indicate the width of the Rydberg-atom velocity distribution, the vertical bars reflect the statistical uncertainty in the measured signals. The solid lines show the results expected on the basis of the Monte Carlo collision model (see text).

PSD (typically ~10–20 μsec depending on the bias applied to the drift region) and its component of velocity in the plane of the PSD, i.e., the xy plane [2,3,14]. Ion-arrival-position distributions at the PSD are therefore directly related to the velocity and angular distributions of the product K^+ ions.

Initial kinematic studies were undertaken using Rydberg atoms having a Maxwellian speed distribution that were excited with the laser incident perpendicular to the potassium atom beam. The K^+-ion-arrival-position distributions observed following $K(55p)$-SF_6 and $K(13p)$-SF_6 collisions are shown in Fig. 3. The Rydberg atoms are initially created in a small volume at $x=y=0$ and are directed along the y axis. Figure 3 also includes the corresponding ion-arrival-position distributions expected on the basis of the Monte Carlo model. At $n=55$, the agreement between the measured and calculated distributions is very good: postattachment electrostatic interactions are negligible and the K^+ ions continue unperturbed along their initial trajectories. In contrast, at $n=13$, strong postattachment electrostatic interactions lead to substantial K^+-ion scattering. This scattering is also evident in the model calculations, but the predicted ion-arrival-position distribution at $n=13$ is not in good agreement with experimental data. In particular, the average y component of velocity of the observed K^+ ions is substantially less than predicted by the model, which again suggests that some mechanism (not included in the model) is operative that enhances free-ion production at low Rydberg-atom velocities.

To further explore this discrepancy, ion-arrival-position distributions were recorded at $n=13$ using velocity-selected Rydberg atoms. These results, obtained with nominal Rydberg-atom velocities of 820, 520, and 270 m sec^{-1}, are shown in Fig. 4 together with the corresponding model predictions. Model and experiment agree quite well at the two higher velocities, although differences remain at the lowest velocity where the model predicts that the average y component of velocity of the detected K^+ ions will be opposite in direction to that of the parent Rydberg atoms. This results because (in the absence of internal-to-translational energy transfer) only for those collisions in which the initial Rydberg atom and SF_6 velocities are oppositely directed will the kinetic energy of relative motion of the ion pair be sufficient to allow them a significantly probability of escape. The K^+ ion, however, receives substantial momentum from the SF_6^- ion before separation occurs and is, on average, scattered in the backward direction. The observation that the average y component of K^+-ion velocity is not negative lends further support to the idea that some

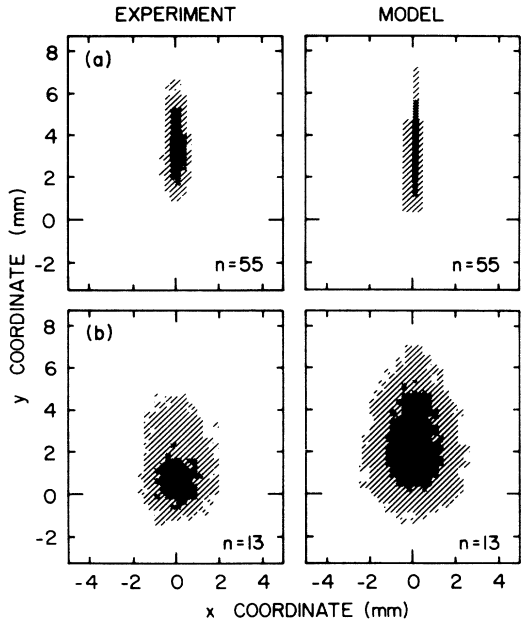

FIG. 3. Observed and predicted K^+-ion-arrival-position distributions following (a) $K(55p)$-SF_6 and (b) $K(13p)$-SF_6 collisions. The Rydberg atoms have a Maxwellian speed distribution and are initially created in a small volume at $x=y=0$ directed along the y axis. The gray scale indicates the relative ion signal count rates at different elements of the PSD surface expressed as a percentage of the peak count rate and correspond to the ranges 100–70 %, 70–40 %, and 40–10 %.

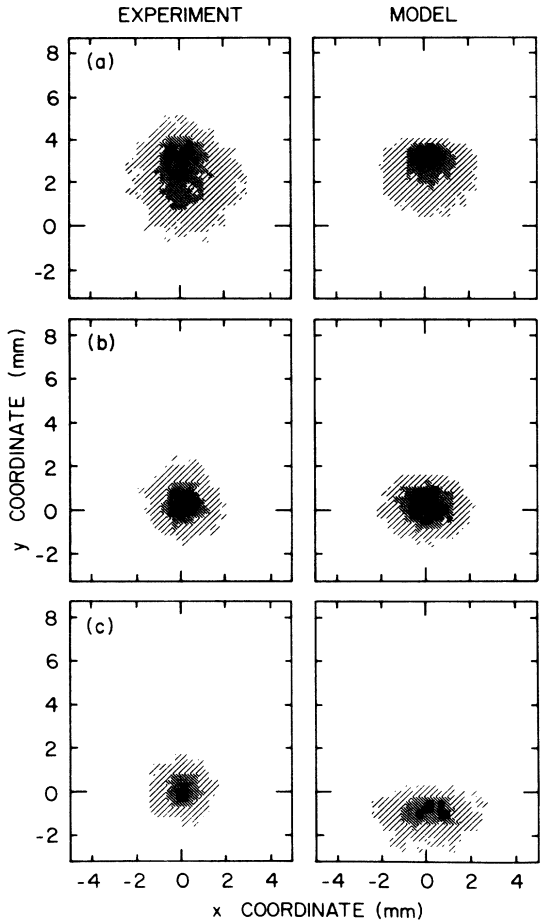

FIG. 4. Observed and predicted K^+-ion-arrival-position distributions following $K(13p)$-SF_6 collisions for nominal Rydberg-atom velocities of (a) 820, (b) 520, and (c) 270 m sec^{-1}. Other initial conditions and the gray scale are as in Fig. 3.

postattachment interaction occurs which provides additional translational energy to the product ion pairs to assist in their separation.

The present data strongly suggest that, following Rydberg electron transfer in K(np)-SF_6 collisions at low-to-intermediate n, internal energy from the product SF_6^{-*} ion may be transferred into translation. A similar energy transfer has been hypothesized previously to explain why the lifetimes of SF_6^{-*} ions formed in low-n collisions are longer than those of ions formed in high-n collisions [15], and might also help explain the unusual velocity dependence recently observed in He(14^1P)-SF_6 collisions [16]. The precise mechanism by which energy interchange occurs is not revealed in the present work, but if it occurs through a close collision it is remarkable that energy transfer can occur without charge transfer and mutual ion-ion neutralization. Nonetheless, comparison of the experimental data and model calculations in Fig. 2(a) suggests that approximately one-third of the ion pairs formed at the lowest collision velocities undergo energy transfer and separate as free ions. The energy interchange, however, need not be particularly efficient because an energy transfer of only ~ 20 meV [which is comparable to the vibrational spacings in SF_6 and (presumably) SF_6^{-*}] is sufficient to account for the present observations, whereas the total internal energy of the SF_6^{-*} ions is ~ 1 eV. A thorough understanding of the energy-transfer process, however, will require a detailed investigation of the nature and dynamical behavior of the bound ion pairs.

This research is supported by the National Science Foundation under Grant No. PHY-8709637 and by the Robert A. Welch Foundation.

[1] F. B. Dunning, J. Phys. Chem. **91**, 2244 (1987).
[2] C. W. Walter, K. A. Smith, and F. B. Dunning, J. Chem. Phys. **90**, 1652 (1989).
[3] X. Ling, M. A. Durham, A. Kalamarides, R. W. Marawar, B. G. Lindsay, K. A. Smith, and F. B. Dunning, J. Chem. Phys. **93**, 8669 (1990).
[4] For a discussion of the free-electron model, see, for example, the articles of M. Matsuzawa and A. P. Hickman, R. E. Olson, and J. Pascale, in *Rydberg States of Atoms and Molecules,* edited by R. F. Stebbings and F. B. Dunning (Cambridge University Press, New York, 1983).
[5] Z. Zheng, K. A. Smith, and F. B. Dunning, J. Chem. Phys. **89**, 6295 (1988).
[6] H. S. Carman, Jr., C. E. Klots, and R. N. Compton, J. Chem. Phys. **90**, 2580 (1989).
[7] K. Harth, M.-W. Ruf, and H. Hotop, Z. Phys. D **14**, 149 (1989).
[8] I. M. Beterov, G. L. Vasilenko, I. I. Riabstev, B. M. Smirnov, and N. V. Fateyev, Z. Phys. D **6**, 55 (1987).
[9] B. G. Lindsay, K. A. Smith, and F. B. Dunning, Rev. Sci. Instrum. **62**, 1656 (1991).
[10] See, for example, Y. Wang and J. Weiner, Phys. Rev. A **42**, 675 (1990)
[11] T. H. Jeys, G. B. McMillian, K. A. Smith, F. B. Dunning, and R. F. Stebbings, Phys. Rev. A **26**, 335 (1982).
[12] J. P. McIntire, G. B. McMillian, K. A. Smith, F. B. Dunning, and R. F. Stebbings, Phys. Rev. A **29**, 381 (1984); L. N. Goeller, G. B. McMillian, K. A. Smith, and F. B. Dunning, *ibid.* **30**, 2756 (1984).
[13] W. P. Spencer, A. G. Vaidyanathan, D. Kleppner, and T. W. Ducas, Phys. Rev. A **26**, 1490 (1982).
[14] C. W. Walter, B. G. Lindsay, K. A. Smith, and F. B. Dunning, Chem. Phys. Lett. **154**, 409 (1989).
[15] G. Brincourt, S. Rajab Pacha, R. Catella, Y. Zerega, and J. André, Chem. Phys. Lett. **156**, 573 (1989).
[16] A. Pesnelle, C. Ronge, M. Perdrix, and G. Watel, Phys. Rev. A **42**, 273 (1990).

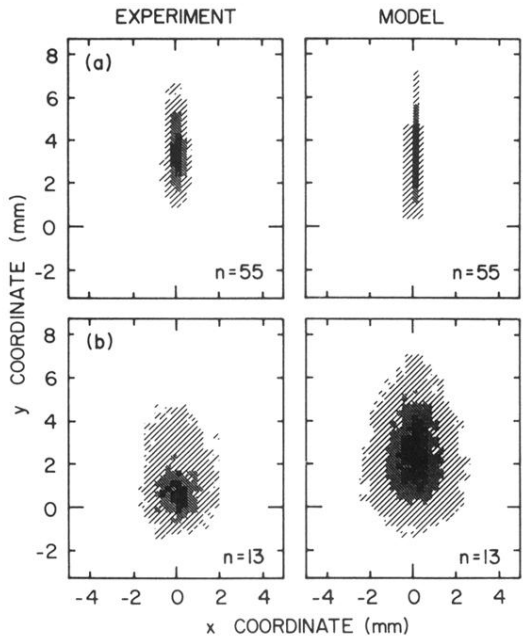

FIG. 3. Observed and predicted K^+-ion-arrival-position distributions following (a) $K(55p)$-SF_6 and (b) $K(13p)$-SF_6 collisions. The Rydberg atoms have a Maxwellian speed distribution and are initially created in a small volume at $x=y=0$ directed along the y axis. The gray scale indicates the relative ion signal count rates at different elements of the PSD surface expressed as a percentage of the peak count rate and correspond to the ranges 100–70 %, 70–40 %, and 40–10 %.

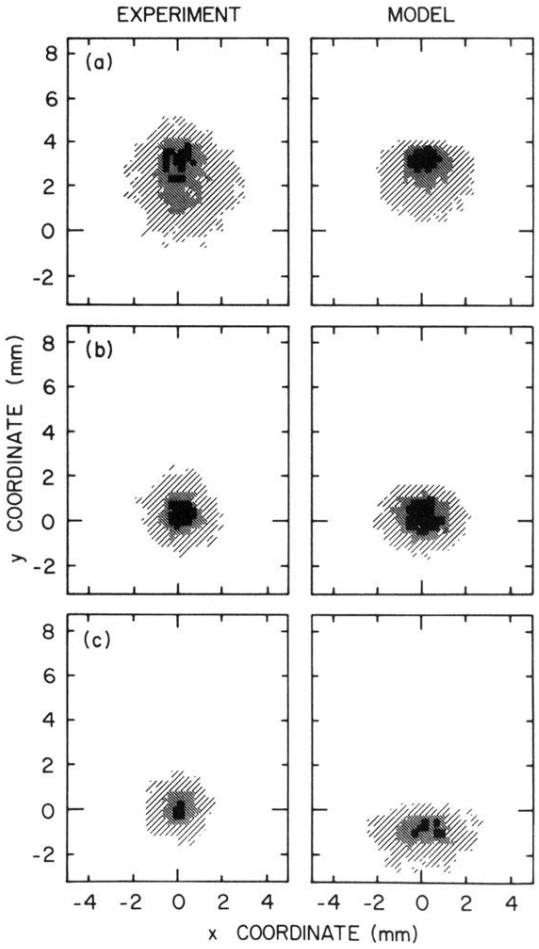

FIG. 4. Observed and predicted K^+-ion-arrival-position distributions following $K(13p)$-SF_6 collisions for nominal Rydberg-atom velocities of (a) 820, (b) 520, and (c) 270 m sec^{-1}. Other initial conditions and the gray scale are as in Fig. 3.